New Chemical Method of Obtaining Thick $Ga_{1-x}Mn_xN$ Layers: Prospective Spintronic Material

Michal Kaminski,*,† Slawomir Podsiadlo,† Pawel Dominik,† Krzysztof Wozniak,‡ Lukasz Dobrzycki,‡ Rafal Jakiela,§ Adam Barcz,§,|| Marek Psoda,⊥ Jaroslaw Mizera,⊥ Rajmund Bacewicz,# Marcin Zajac,@ and Andrzej Twardowski@

Faculty of Chemistry, Warsaw University of Technology, Noakowskiego 3, 00-664 Warsaw, Poland, Chemistry Department, Warsaw University, Pasteura 1, 02-093 Warsaw, Poland, Institute of Physics and Institute of Electron Technology, Polish Academy of Sciences, Al. Lotnikow 32/46, 02-668 Warsaw, Poland, Faculty of Materials Science and Engineering, Warsaw University of Technology, Woloska 141, 02-507 Warsaw, Poland, Institute of Physics, Warsaw University of Technology, Koszykowa 75, 00-662 Warsaw, Poland, and Institute of Physics, Warsaw University, Hoza 69, 00-681 Warsaw, Poland

Received October 14, 2006. Revised Manuscript Received February 14, 2007

The synthesis and characterization of $Ga_{1-x}Mn_xN$ thick layers are reported. The layers were prepared by the modified sublimation sandwich method (SSM) from GaN powder and powdered Mn sources and reacted with ammonia. $Ga_{1-x}Mn_xN$ layers having a current maximum size of 60 μm thickness and 10 mm × 10 mm area were obtained. The crystals of best crystalline quality were obtained with a growth rate of 25 μm/h. SIMS measurements showed the presence of layers containing up to 4 atom % Mn. Measurements involving X-ray diffraction (structure refinement), rocking curves, map of reflections, and EXAFS confirmed good structural properties without phase separation. The measurements carried out by a superconducting quantum interferometer showed that the material revealed typical paramagnetic properties.

Introduction

A rapid development of GaN-based semiconductors has taken place in recent years. GaN is applied in blue light emitting diodes and lasers, and $Ga_{1-x}Mn_xN$ is a prospective material for spintronics.[1−3] Gallium nitride doped with magnetic elements such as manganese exhibits ferromagnetic properties at ambient temperatures.[4,5] In our earlier work, we succeeded in obtaining bulk $Ga_{1-x}Mn_xN$ and Ga(Mn,Si)N single crystals that, were small and suitable for scientific research only.[2,6] Mn-doped GaN layers of good quality can be obtained by various methods among which the most important are molecular beam epitaxy (MBE),[5,7−10] metalloorganic chemical vapor deposition (MOCVD),[11−13] and hydride vapor-phase epitaxy (HVPE).[14,15] The Mn-doped GaN thin films grown by MBE reveal paramagnetic or[10] ferromagnetic[8,9] properties or the coexistence of ferromagnetic and paramagnetic contributions,[7] depending on the Mn concentration and temperature of the measurements. However, the high level of manganese dopant may come from Mn-based compounds or alloys.[16,17] Thin $Ga_{1-x}Mn_xN$ MOCVD layers that show ferromagnetic properties are usually co-doped with magnesium and silicon, which are *p*- and *n*-dopants, respectively.[11−13] HVPE allows thick GaN layers to grow.[18] Yu et al.[14] reported 3 μm $Ga_{1-x}Mn_xN$ layers with $x = 0.057$, 0.088, and 0.16. Depending on the HCl−Mn flux, different manganese phases were detected. Whether the

* Corresponding author. Tel.: +48(22)6225185; fax: +48(22)6282741; e-mail: michal@ch.pw.edu.pl.
† Faculty of Chemistry, Warsaw University of Technology.
‡ Chemistry Department, Warsaw University.
§ Institute of Physics, Polish Academy of Sciences.
|| Institute of Electron Technology, Polish Academy of Sciences.
⊥ Faculty of Materials Science and Engineering, Warsaw University of Technology.
Institute of Physics, Warsaw University of Technology.
@ Institute of Physics, Warsaw University.

(1) Nakamura, S. *J. Cryst. Growth* **1997**, *170*, 11.
(2) Podsiadlo, S.; Szyszko, T.; Gebicki, W.; Gosk, J.; Bacewicz, R.; Dobrzycki, L.; Wozniak, K.; Zajac, M.; Twardowski, A. *Chem. Mater.* **2003**, *15* (24), 4533.
(3) Jeon, H. C.; Kang, T. W.; Kim, T. W. *Solid State Commun.* **2004**, *132*, 63.
(4) Dietl, T.; Ohno, H.; Matsukura, F.; Cibert, J.; Ferrand, D. *Science* **2000**, *287*, 1019.
(5) Kane, M. H. et al. *Mater. Sci. Eng., B* **2006**, *126*, 230.
(6) Kaminski, M.; Szyszko, T.; Podsiadlo, S.; Wozniak, K.; Dobrzycki, L.; Gebicki, W.; Gosk, J.; Zajac, M.; Twardowski, A. *J. Cryst. Growth* **2006**, *291*, 12.
(7) Hori, H.; Sonoda, S.; Sasaki, T.; Yamamoto, Y.; Shimizu, S.; Suga, K.; Kindo, K. *Physica B (Amsterdam, Neth.)* **2002**, *324*, 142.
(8) Overberg, M. E.; Abernathy, C. R.; Pearton, S. J.; Theodoropoulou, N. A.; McCarthy, K. T.; Hebard, A. F. *Appl. Phys. Lett.* **2001**, *79*, 1312.
(9) Yoon, I. T.; Park, C. S.; Kim, H. J.; Kim, Y. G.; Kang, T. W.; Jeong, M. C.; Ham, M. H.; Myoung, J. M. *J. Appl. Phys.* **2004**, *95*, 591.
(10) Kondo, T.; Kuwabara, S.; Owa, H.; Munekata, H. *J. Cryst. Growth* **2002**, *237*, 1353.
(11) Reed, M. J.; Arkun, F. E.; Berkman, E. A.; Elmasry, N. A.; Zavada, J.; Luen, M. O.; Reed, M. L.; Bedair, S. M. *Appl. Phys. Lett.* **2005**, *86*, 102504.
(12) Kane, M. H.; et al. *Semicond. Sci. Technol.* **2005**, *20*, 5.
(13) Kane, M. H.; et. al. *J. Cryst. Growth* **2006**, *287*, 591.
(14) Yu, Y. Y.; Zhang, R.; Xiu, X. Q.; Xie, Z. L.; Yu, H. Q.; Shi, Y.; Shen, B.; Gu, S. L.; Zheng, Y. D. *J. Cryst. Growth* **2004**, *269*, 270.
(15) Xiu, X. Q.; Zhang, R.; Li, B. B.; Xie, Z. L.; Chen, L.; Liu, B.; Han, P.; Gu, S. L.; Shi, Y.; Zheng, Y. D. *J. Cryst. Growth* **2006**, *292*, 212.
(16) Yoon, I. T.; Kang, T. W.; Kim, D. J. *Mater. Sci. Eng., B* **2006**, *134*, 49.
(17) Hashimoto, M.; Zhou, Y. K.; Tampo, H.; Kanamura, M.; Asahi, H. *J. Cryst. Growth* **2003**, *252*, 499.
(18) Hermann, M.; Gogova, D.; Siche, D.; Schmidbauer, M.; Monemar, B.; Stutzmann, M.; Eickhoff, M. *J. Cryst. Growth* **2006**, *293*, 462.

10.1021/cm062459j CCC: $37.00
Published on Web 05/27/2007

observed ferromagnetism comes from $Ga_{1-x}Mn_xN$ or Mn-based compounds was not able to be analyzed or confirmed. Xiu et al.[15] obtained a 50 μm thick $Ga_{1-x}Mn_xN$ layer in 30 min deposition time. The analyses confirmed that the material was good without the formation of Mn precipitates or phase separation; however, it exhibited paramagnetic properties.

Here, we report a new method for obtaining layers of $Ga_{1-x}Mn_xN$ by the modified sublimation sandwich method (SSM). This method is well-known, but according to our knowledge, there are no reports on growing $Ga_{1-x}Mn_xN$ by SSM. In fact, SSM is the simplest chemical method of gas-phase transport. SSM is inexpensive and does not require high pressure nor hazardous reacting substances. Some appropriate size layers can be used as free-standing bulk crystals after separating them from the substrate.

Experimental Procedures

Synthesis. Experiments were run in a horizontal tubular quartz reactor. As the heating element, we used a graphite cylinder that was heated by rf induction. Sapphire with a 3 μm GaN thin film grown by MOCVD was used as the substrate. To ensure Ga and Mn transfer, a temperature gradient was employed between the Ga and Mn sources and the substrate ($\Delta T = 70$ °C). $Ga_{1-x}Mn_xN$ layers were grown from the mixtures of GaN powder and powdered Mn. Ga and Mn sources were placed in a quartz boat on top of the graphite. The substrate was positioned 5 mm above the mixture. $Ga_{1-x}Mn_xN$ layers were obtained under the following conditions: temperature 1050−1180 °C, ammonia flow rate 0.2−1.4 l min^{-1}, heating time 5−120 min, and concentration of manganese in the reaction mixture 0.5−10%, relative to the GaN powder weight. As a consequence of the higher (7.5−10%) Mn concentration in the mixture, the material obtained was polycrystalline.

X-ray. Data collection of scattered X-rays was accomplished on a KM4CCD κ-axis diffractometer with graphite-monochromated Mo Kα radiation. The crystal was positioned at 62 mm from the CCD camera. Frames totaling 1877 were measured at 1.25° intervals with a counting time of 5 or 28 s depending on the detector position. The data were corrected for Lorentzian and polarization effects. Analytical correction for absorption was applied.[19] Data reduction and analysis were carried out with the Oxford diffraction programs.[20] The structure was solved by direct methods[21] and refined using SHELXL.[22] The refinement was based on F^2 for all reflections except those with a very negative F^2 value. Weighted R factors wR and all GOF S values were based on F^2. Conventional R factors were based on F with F set to zero for negative F^2. The $F_o^2 > 2\sigma(F_o^2)$ criterion was used only for calculating R factors and is not relevant to the choice of reflections for the refinement. The R factors based on F^2 were about twice as large as those based on F. Scattering factors were taken from Tables 6.1.1.4 and 4.2.4.2 in ref 23.

Rocking Curves and Map of Reflections. Measurements were done using an X-ray diffractometer D8 Discover Series 2 by Bruker AXS. The rocking curves and map of reflections from the (002) planes were determined. The X-ray diameter was 0.1 mm × 5 mm, and the studied area had a diameter of 5 mm. There were 72 scans for every layer (step size 5°). There were no differences between these 72 rocking curves, so only one for the buffer layer and one for GaN by SSM were chosen to show in this study.

SIMS. Measurements were performed using a CAMECA IMS6F microanalyzer. Ga, N, and Mn measurements were performed with an oxygen (O_2^+) primary beam, with the beam current kept at 800 nA. The size of the eroded crater was about 150 μm × 150 μm, and the secondary ions were collected from a central region of 30 μm in diameter. H, C, O, and Si measurements were performed with a Cs^+ primary beam, with the beam current kept at 170 nA. The secondary ions were collected from a region 30 μm in diameter.

Superconducting Quantum Interference Device (SQUID). Magnetic properties were studied by a SQUID manufactured by Cryogenic.

EXAFS. The κ-edge absorption of manganese was measured at the HASYLAB synchrotron facility in Hamburg (A1 beamline). A two-crystal Si (111) monochromator with a resolution of 1 eV at 8 keV was employed. Measurements were carried out in fluorescence mode using the seven-element Si/Li detector. Samples were kept at liquid nitrogen temperature to minimize thermal disorder.

Results and Discussion

The size of layers obtained was ca. 10 mm × 10 mm. The layers varied in color from light amber to dark amber depending on the Mn concentration, and the thickness of the layers was 2−60 μm, which varied with the difference of reaction time, temperature, and ammonia flow rate. Layers with the best crystalline quality were obtained after a deposition time of 15−60 min. Their thickness varied from 4 to 28 μm. A series of experiments showed that temperatures below 1050 °C did not result in the preparation of $Ga_{1-x}Mn_xN$ layers. The upper limit of the process temperature was 1180 °C since a decomposition of $Ga_{1-x}Mn_xN$ was observed. The lower ammonia flow rates (0.2−0.6 l min^{-1}) resulted in the best crystalline quality, while flow rates within the range of 1−1.2 L min^{-1} produced only 2 μm thick layers of very poor quality. We also observed that the concentration of Mn in the reaction mixture in the range of 0.5−7% did not have an effect on the growth rate. Therefore, the optimum growth parameters were as follows: time, 15−60 min; temperature, 1110−1140 °C; ammonia flow rate, 0.2−0.6 l min^{-1}; and initial amount of manganese introduced into the reaction mixture, −2.5% by weight. We have also found that the materials of best crystalline quality were obtained with a growth rate of 25 μm/h. Samples prepared in these conditions are the subject of studies presented in this manuscript. Figure 1 presents a photograph of the $Ga_{1-x}Mn_xN$ layer.

The crystal structure of $Ga_{1-x}Mn_xN$ ($x = 0.04$) layers is illustrated in Figure 2. Doped GaN−similar to the pure one−crystallizes in the same polar $P6(3)mc$ (No. 186) space group from the hexagonal crystal system forming a layered structure of Wurtzite 2H type. In such a crystal structure, cations and anions form separate layers perpendicular to the 6-fold axis. Because of the small amount of doping agent, the positions and atomic displacement parameters (ADPs) of Ga and Mn ions were refined as identical for both species. As compared

(19) CrysAlis RED, Oxford Diffraction Ltd., version 1.171.28cycle2 beta. Analytical numeric absorption correction using a multifaceted crystal model based on expressions derived by R. C. Clark and J. S. Reid.
(20) CrysAlis CCD, Oxford Diffraction Ltd., version 1.171.28cycle2 beta.
(21) Sheldrick, G. M. *Acta Crystallogr., Sect. A: Found. Crystallogr.* **1990**, *46*, 467.
(22) Sheldrick, G. M. *SHELXL93*, Program for the Refinement of Crystal Structures; University of Göttingen: Göttingen, Germany.
(23) *International Tables for Crystallography*; Wilson, A. J. C., Ed.; Kluwer: Dordrecht, The Netherlands, 1992; Vol. C.

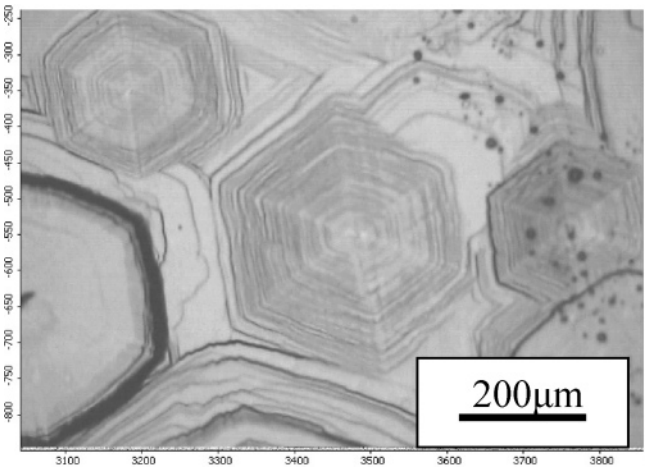

Figure 1. Photograph of $Ga_{1-x}Mn_xN$ layer.

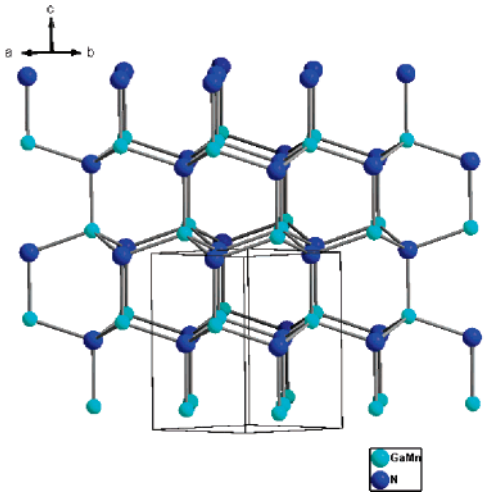

Figure 2. Structure of Mn-doped GaN layer.

to pure GaN data[24,25] (a = 3.1891(1) Å and c = 5.1853(3) Å and a = 3.190(1) Å and c = 5.189(1) Å), the unit cell parameters of the doped sample (a = 3.1932(15)Å and c = 5.185(3)Å) are very similar to those obtained for pure GaN. The shortest interatomic distances between nitrogen and gallium ions are equal to 1.9503(10) and 1.956(2) Å with valence angles N−Ga−N equal to 109.89(5) and 109.04-(5)°. Crystal data and experimental details for the doped GaN/Mn(4%) layers are given in ref 26.

The high quality of the crystalline structure was also confirmed by rocking curve analysis and map of reflections. Both MOCVD GaN buffer thin film and $Ga_{1-x}Mn_xN$ grown with SSM were investigated. Rocking curve and map of reflections for buffer GaN and layers grown with SSM are shown in Figures 3 and 4, respectively.

In the first case, the full width at half- maximum (fwhm) value was 0.129° for the (002) reflection, and the maximum on the map of reflection was observed at 2θ = 34.570°. The X-ray rocking curve of the $Ga_{1-x}Mn_xN$ layer has a fwhm of 0.097° for (002) with the maximum of the signal for 2θ = 34.580°.

By comparing these values, one can say that there are no large differences between the crystalline structure of the buffer GaN and the obtained $Ga_{1-x}Mn_xN$ structure. Moreover, the lower value of fwhm in the doped sample proves that the crystal structure of our $Ga_{1-x}Mn_xN$ layer is better than that of buffer GaN. Because of the fact that buffer GaN was grown heteroepitaxially on sapphire and the lattice constant mismatches Al_2O_3 with GaN, a high dislocation density and defects in the GaN epitaxial film occur.[27] In our layer, there was only one peak, which means that only one single phase was detected with no secondary phase formation. Also, the lack of broadening or separating of the rocking curve peak, as well as the appearance of only one maximum on the map of reflections, testifies that there is no twinning nor significant mosaicity of the material. However, some differences can be seen in the 2-D shape of the equivalent reflections. A slightly elongated shape of the reflection in the *X* direction probably is a consequence of manganese doping, which replaces Ga sites and in which the atomic radius differs from gallium.

Secondary ion mass spectrometry (SIMS) measurements were accomplished to check the manganese concentration as well as the distribution of gallium, nitrogen, and impurities—such as hydrogen, carbon, oxygen, and silicon—in $Ga_{1-x}Mn_xN$ layers. Concentration profiles of Ga, Mn, and N are shown in Figure 5. The Mn content in the $Ga_{1-x}Mn_xN$ layers calculated from the Mn concentration amounted to ∼4 atom %. The influence of temperature, ammonia flow rate, and manganese concentration in the substrate material on the doping level of the obtained $Ga_{1-x}Mn_xN$ layers will be discussed elsewhere. Ga nad N signals decreased on the $Ga_{1-x}Mn_xN$/GaN interface. This presumably comes from a matrix effect or sample charging due to a higher resistivity of the GaN layer. Generally, the concentration of the main species—gallium, manganese, and nitrogen—is the same and in equal proportion for the whole cross-section of the layer. This proves good quality of the layers obtained. Concentration profiles of impurities are shown in Figure 6. High concentrations of hydrogen, carbon, oxygen, and silicon at the beginning and the end of the profiles are a result of surface and GaN/Al_2O_3 interface contamination, respectively. The concentration of impurities drops rapidly away from the surface down to about 10^{17} cm^{-3} for Si and C and 10^{18} to 10^{19} cm^{-3} for O and H.

Investigation of X-ray absorption fine structure is a direct atom selective method for probing the local order in solids. In this study, we have measured and analyzed the extent of

(24) Chen, X.-L.; Lan, Y.-C.; Liang, J.-K.; Cheng, X.-R.; Xu, Y.-P.; Xu, T.; Jiang, P.-Z.; Lu, K.-Q. *Chin. Phys. Lett.* **1999**, *16*, 107.
(25) Schulz, H.; Thiemann, K. H. *Solid State Commun.* **1977**, *23*, 815.
(26) Crystal data for $Ga_{1-x}Mn_xN$ layers: empirical formula $Ga_{0.96}Mn_{0.04}N$, fw 83.14, temp 100(2) K, wavelength Mo Kα = 0.71073 Å, hexagonal system, *P*6(3)*mc* (*v* 186), a = 3.1932(15) Å, c = 5.185(3) Å, V = 45.79(4) Å^3, Z = 2, d_{calcd} = 6.030 mg/m^3, abs coeff = 28.290 mm^{-1}, $F(000)$ = 75.5, crystal size = 0.18 mm × 0.11 mm × 0.02 mm, θ range = 7.36−44.31°, $-6 \le h \le 6$, $-6 \le k \le 6$, $-10 \le l \le 10$, reflns collected/unique = 2057/165 [R(int) = 0.0207], completeness to θ = 36.33° = 94.9%, analytical abs correction, max and min transmission 0.62 and 0.004, full matrix least-squares on F^2, data/restraints/parameters = 165:1:8, GOF on F^2 =1.320, final R indices [$I > 2\sigma(I)$]: R1 = 0.0084, wR2 = 0.0198, R indices (all data): R1 = 0.0111, wR2 = 0.0201, absolute structure parameter = 0.03(3), extinction coeff = 0.030(2), largest diff peak and hole = 0.375 and −0.709 e Å^{-3}, respectively.
(27) Ponce F. A. In *Group III Nitride Semiconductor Compounds*; Gil, B., Ed.; Oxford University Press: Oxford, 1998; p 123.

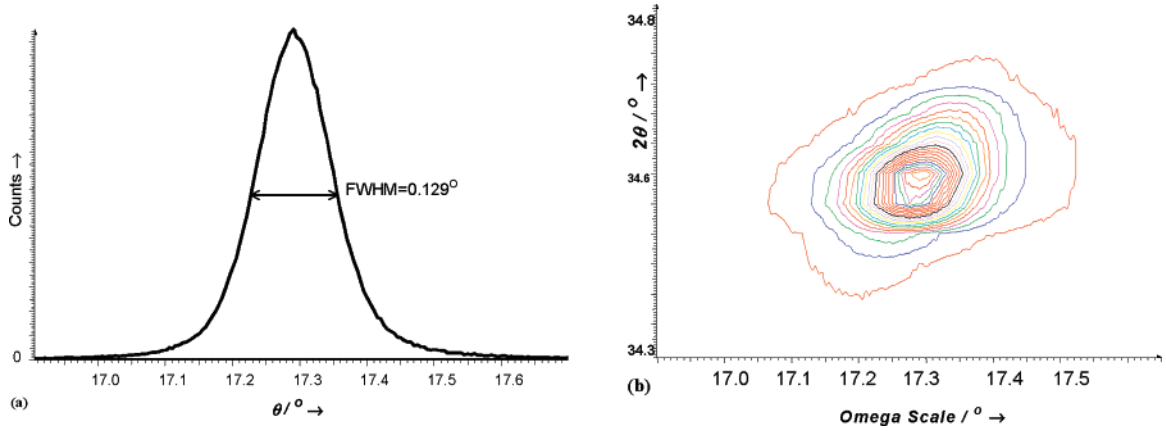

Figure 3. (a) Rocking curve for buffer GaN and (b) 2-D map of reflection for buffer GaN.

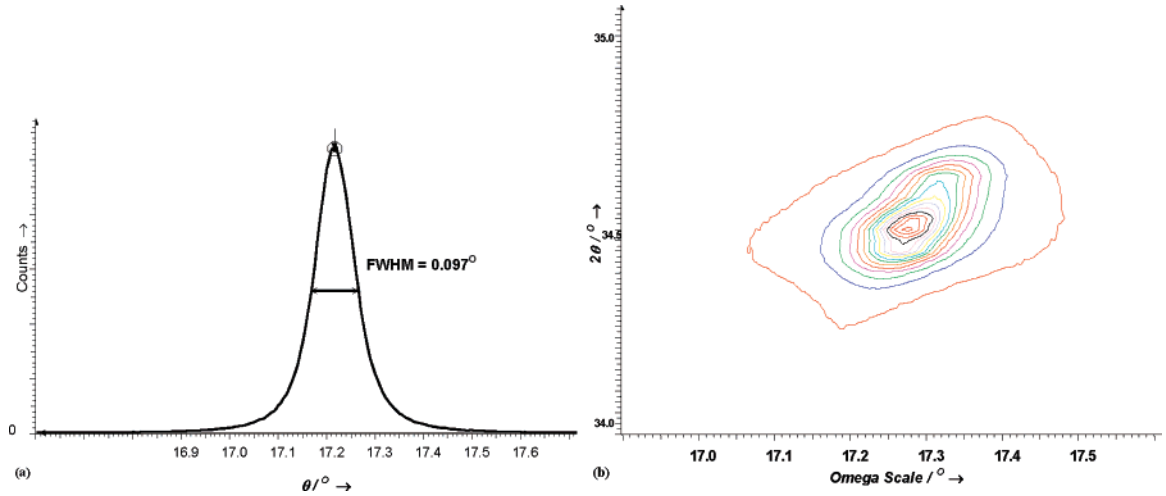

Figure 4. (a) Rocking curve for $Ga_{1-x}Mn_xN$ grown by SSM and (b) 2-D map of reflection for $Ga_{1-x}Mn_xN$ grown by SSM.

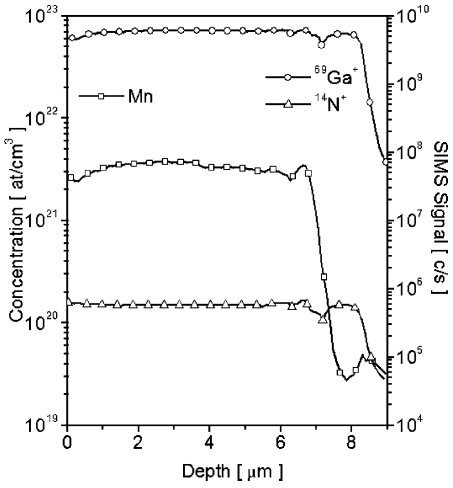

Figure 5. Mn concentration profile and Ga and N profiles as measured by SIMS.

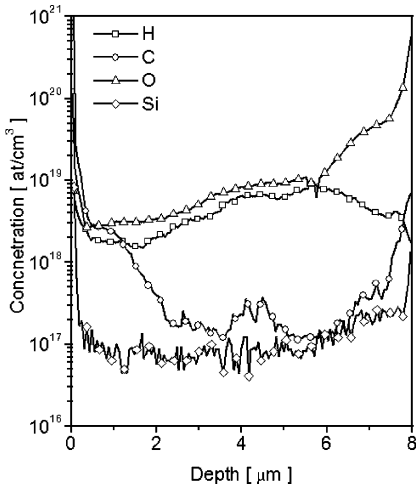

Figure 6. H, C, O, and Si concentration profiles obtained by SIMS.

the EXAFS at the κ-edge of Mn. This provides information on the local environment of Mn atoms in the GaN host lattice. We refined a model with Mn substituting the Ga site (Mn_{Ga}). The fitting was performed using an ARTEMIS program including multiple scattering paths of photoelectrons. We used scattering amplitudes and phases calculated with the FEFF8 program. The results obtained for the sample with 2% Mn are shown in Figure 7. This presents Fourier transformed EXAFS oscillation data together with a fitted line for the Mn_{Ga} site. A very good agreement was obtained up to 7 Å from the Mn atom (10 coordination shells). This signifies that a local environment of the Mn atom closely resembles that of the Ga host atoms. The nearest-neighbor distance R_{Mn-N} is 1.98 ± 0.01 Å, which is only 1.5% longer than the equivalent Ga−N bond length. Differences for higher coordination shell radii do not exceed 1%. However, the Debye−Waller factor for the nearest-neighbor shell is $\sigma^2 = 0.006$ Å^2, which is larger than that for single (Ga,-Mn)N crystals grown from the gas phase (0.0033 Å^2).[28]

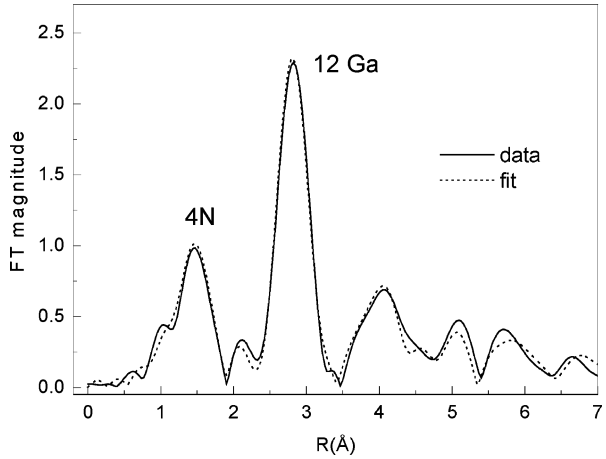

Figure 7. Fourier transforms of EXAFS oscillation (Ga,Mn)N layer with 2% Mn. Solid line: data and dotted line: substitutional Mn_{Ga} model.

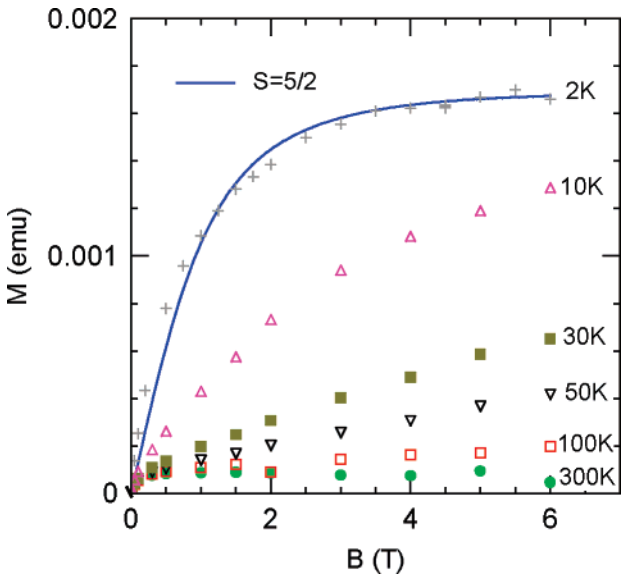

Figure 8. Magnetic moment of $Ga_{1-x}Mn_xN$ layer plotted as a function of magnetic field at various temperatures. The solid line corresponds to the Brillouin function fit with $S = 5/2$.

The magnetization of $Ga_{1-x}Mn_xN$ was measured using a SQUID magnetometer as a function of temperature (2−300 K) and magnetic field (0−6 T). The results were corrected for the diamagnetic contribution of the sapphire substrate and $Ga_{1-x}Mn_xN$ layer. In general, an overall paramagnetic behavior was observed, which can be assigned to a system of non-interacting magnetic moments associated with Mn ions substituting the Ga sites in the GaN lattice. The magnetic measurements revealed a pronounced tendency to saturation at 2 K and a linear magnetic field dependence at higher temperatures (Figure 8). The data can be described by classical Brillouin function (depicted by the solid curve) with spin $S = 5/2$, which corresponds to a Mn^{2+} (d^5) configuration. A very small deviation from the fit may be due to the antiferromagnetic coupling between Mn ions in $Ga_{1-x}Mn_xN$ observed earlier.[29]

(28) Bacewicz, R.; Filipowicz, J.; Podsiadlo, S.; Szyszko, T.; Kaminski, M. *J. Phys. Chem. Solids* **2003**, *64*, 1469.
(29) Zajac, M.; Gosk, J.; Kaminska, M.; Twardowski, A.; Szyszko, T.; Podsiadlo, S. *Appl. Phys. Lett.* **2001**, *79*, 2432.

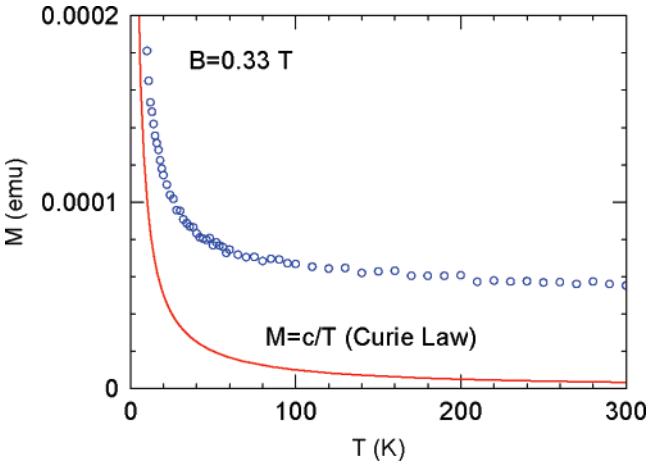

Figure 9. Temperature dependence of magnetization (solid line represents schematically the Curie law).

The temperature dependence of magnetization, shown in Figure 9, does not follow the Curie law (characteristic for pure paramagnetic materials). This can be understood by the existence of a very small, temperature-independent ferromagnetic component that shifts the hyperbolic curve by a constant value. This ferromagnetic component is visible even at 300 K, so the critical temperature of this ferromagnetic component is well above room temperature. Its exact value is above the available experimental range (2−300 K), so it cannot be determined. This ferromagnetic contribution most probably results from Mn-based precipitates formed during crystal growth.

Conclusion

In summary, we have grown single crystalline layers by the SSM system. The presented method is inexpensive, simple, and fast. It does not require high pressure nor complicated laboratory systems. The use of simple substances is one of the advantages. Analyses by X-ray, rocking curves, map of reflections, and EXAFS indicated that these layers were homogeneous without Mn precipitates and that the Mn atoms were substituted for Ga sites. In general, an overall paramagnetic behavior was observed. The origin of the small ferromagnetic component is unclear. Further improvement of the system could take effect in obtaining layers of larger size, dependent on size of the substrate used, size of the reactor (e.g., amount of gallium source, free path between GaN/Mn mixture, and substrate), and reaction time. A significant increase in thickness can result in the possibility of separating the layers from the substrate. Also, additional codopants in the form of magnesium and silicon could produce a ferromagnetic material.

Acknowledgment. This work was supported by the State Committee for Scientific Research (Grant 3T09B 056 28).

Supporting Information Available: Crystallographic information file. This material is available free of charge via the Internet at http://pubs.acs.org.

CM062459J